ORIGINAL ARTICLE

Improving Image Correlation and Differentiation of 3D Endoluminal Lesions in the Air Spaces Using a Novel Target Gray Level Mapping Technique: A Preliminary Study of Its Application to Computed Tomographic Colonography and Comparison with Traditional Surface Rendering Method

Lih-Shyang Chen[1] · Ta-Wen Hsu[2,3] · Shao-Jer Chen[3,4,9] · Shu-Han Chang[1] · Chih-Wen Lin[3,4] · Yu-Ruei Chen[3,4] · Chin-Chiang Hsieh[5] · Shu-Chen Han[6] · Ku-Yaw Chang[7] · Chun-Ju Hou[8]

Abstract

Purpose To improve the three dimensional (3D) and two dimensional (2D) image correlation and differentiation of 3D endoluminal lesions in the traditional surface rendering (SR) computed tomographic endoscopy (CTE), a target gray level mapping (TGM) technique is developed and applied to computed tomographic colonography (CTC) in this study.

Methods A study of sixty-two various endoluminal lesions from thirty patients (13 males, 17 females; age range 31–90 years) was approved by our institutional review board and evaluated retrospectively. The endoluminal lesions were segmented using gray level threshold. The marching cubes algorithm was used to detect isosurfaces in the segmented volumetric data sets. TGM allows users to interactively apply grey level mapping (GM) to region of interest (ROI) in the 3D CTC. Radiologists conducted the clinical evaluation and the resulting data were analyzed.

Results TGM and GM are significantly superior to SR in terms of surface texture, 3D shape, the confidence of 3D to 2D, 2D to 3D image correlation, and clinical classification of endoluminal lesions (P < 0.01). The specificity and diagnostic accuracy of GM and TGM methods are significantly better than those of SR (P < 0.01). Moreover, TGM performs better than GM (specificity: 75.0–85.7% vs. 53.6–64.3%; accuracy: 88.7–93.5% vs. 77.4–83.9%). TGM is a preferable display mode for further localization and differentiation of a lesion in CTC navigation.

Conclusions Compared with only the spatial shape information in traditional SR of CTC images, the 3D shapes and gray level information of endoluminal lesions can be provided by TGM simultaneously. 3D to 2D image correlations are also increased and facilitated at the same time. TGM is less affected by adjacent colon surfaces than GM. TGM serves as a better way to improve the image correlation and differentiation of endoluminal lesions.

Keywords Image processing · Computer-assisted · Tomography · X-ray computed · CT colonography · Colonic neoplasms · Imaging · Three-dimensional

1 Introduction

There are many tubular structures which transport food, air and blood within the human body in order to support life. However, a great many infectious, toxigenic or oncogenic sources easily get into the human body through these tubular structures. For this reason, endoluminal lesions are common medical problems. For example, the recent coronavirus disease (COVID-19) outbreak is due to a viral infection, most commonly entering through the airway. The outbreak now greatly threatens human lives and societies. Colorectal cancer is another common form of endoluminal disease and a leading cause of cancer-related death in the world. In the United States, in 2017, there were projected to be 135,430 individuals newly diagnosed with colorectal cancer and 50,260 deaths from the disease [1]. The lifetime risk of colorectal cancer is similar among males and females (4.6%

✉ Shao-Jer Chen
  A120930@tzuchi.com.tw

Extended author information available on the last page of the article

vs 4.2%) [1]. If colorectal cancer is detected at a localized stage, the 5-year survival rate is 90%. Once the cancer has developed distant metastases, the 5-year survival rate is 14% [1].

Traditional optical endoscopy is the first choice for the diagnosis and management of endoluminal lesions; however, it is associated with some limitations. The endoscope is unable to pass through very stenotic and tortuous areas in order to examine the lesions distal to the above areas. The endoscope cannot fully evaluate the lesion below the luminal surface and its extraluminal extension. Additionally, the endoscope is intolerable for some patients. There are also risks of perforation, hemorrhage, infection, and even death [2]. On the contrary, CTE allows the visualization of lesions hidden beyond a stenosis/tortuous area or beneath the surface, and is a noninvasive procedure with a low risk of perforation, hemorrhage, or infection. CTE is an important computer-based alternative to optical endoscopy.

SR is the traditional rendering technique used in CTE. In a routine SR image, the voxel information is simply used for surface estimation and 3D shape visualization [3]. No gray level information of the surface of the endoluminal colon lesion is displayed for differentiation.

Volume rendering (VR) is commonly used in the current commercial CTE systems. VR assigns blue, green, red, and white color channels, respectively, and introduces a transparency function to areas of increasing attenuation [4]. As a result, the final VR images may be very confusing and difficult to interpret.

However, there is a great deal of original gray level information such as air, fat, contrast, calcification densities in the 2D images. Those gray level changes cannot be seen in a 3D SR or VR image. For this reason, CTC interpretation requires radiologists to interactively view 3D and 2D images of the colonic lumen, going back and forth to achieve an accurate diagnosis [5]. Even after spending a lot of time for 3D and 2D image correlation, the readers may still not be sure of the point-to-point correlation between 2D and its corresponding SR or volume rendering images and should image 3D gray level spatial distribution due to lack of 3D to 2D gray level linkage. Therefore, there is a need to improve the commonly used 3D rendering techniques (SR and VR) to facilitate the correlation, and optimize evaluation of, the colonic lumen for polyps and neoplasms.

Chen et al. reported a GM technique that modifies the traditional SR images by applying gray levels to the surface points according to the corresponding grey level values of the original CT images [6]. Because the gray level values mapped in GM technique are the same as original CT images, radiologists and physicians can more easily understand the meaning of the mapping, as opposed to monochrome SR or the abstraction of the translucency transfer function in VR [4, 7].

However, we have found that the GM method should be applied only to lesions or suspicious regions for the identification and differentiation of the 3D surface. This is because if the GM method is applied to the entire 3D surface [6], the grey level surface of the navigation CTC image may appear very complicated, as discussed further in the Results and Discussion sections. As a result, application of the GM method may actually interfere with the analysis of a focal lesion and slow down the navigation process of a complex image.

The purpose of this study is to use the example of CTC in order to develop a better analytic method for 3D endoluminal lesions and to determine how the method facilitates the 2D image correlation and differentiation of 3D endoluminal lesions in comparison with SR images. This study may be extended to other organs with air spaces, such as airway and upper gastrointestinal systems.

2 Materials and Methods

This study is a retrospective study of prospectively acquired data. All patients were transferred due to colon lesions found by colonoscopy and consented to further CT study, operations and pathological examination. They all agreed to receive CTC for better staging of lesions and diagnostic purposes. We studied sixty-two endoluminal lesions from thirty patients, comprised of 13 males and 17 females, with an age range of 31–90 years. The study recruited 34 cases of potential malignancy (11 polyps and 23 cancers) for the index test and 28 cases of other benign conditions (including 17 stools, 3 fluid retention, 2 calcifications/tagging agents and 6 ileocecal valves). All of the case data were compared to the colonoscopic and pathological findings of biopsy or surgery by doctors and pathologists as the gold standard of lesion analysis. Part of the data set (33 endoluminal cases) were used in the Chen article but different from general GM of CTC in that article. TGM was developed in this study to demonstrate 3D shape and gray level information together for more focused and accurate analysis of any interesting area during CTC navigation. This study was approved by our institutional review board.

2.1 Data Acquisition

A spiral CT scan of the patient's abdomen was performed after the entire colon was distended with room air and tagging agent used beforehand (200 ml Telebrix 1-day preparation) [8]. Prone and supine position helical CT scans were performed, 30 s following intravenous contrast administration. The slice thickness of volume data were reconstructed to 1.25 mm. All scans were performed using a 64-slice GE

Lightspeed VCT scanner (GE HealthCare, Milwaukee, Wisconsin, USA).

2.2 Segmentation

The soft tissue of the abdomen and air-distended colon can be completely separated by a defined gray level threshold because colon air is within a narrow range of the CT number, − 1000 Hounsfield units (HUs), in theory. To generate good TGM effect, air areas should be segmented and separated as much as possible.

2.3 Surface Rendering

Marching cubes is an algorithm for generating isosurfaces in volumetric data sets, and has been used to find the surface points of the colon in many CTC applications [9]. The basic concept is that a voxel (cube) can be defined by the values at the eight corners of the cube. The segmented colon surface intersects those cube edges where one vertex is outside the surface and the other is inside the surface. Because of two different symmetries of the cube, there are 15 patterns in which a surface can intersect the cube. By determining which edges of the cube are intersected by the isosurface, triangular patches can be created which divide the cube between regions within the isosurface and regions outside. By connecting the patches from all cubes on the isosurface boundary, a surface representation of the colon is achieved [10].

2.4 Selection of a Target Region of Interest (ROI)

One way to mark the region of interest on a 3D surface is to display a semi-transparent ball in front of the 3D object (endoluminal lesions in our study) and enable the user to use his cursor to control the location of the ball and mark the region of interest (Fig. 1a). The endoluminal surface may go up and down in 3D space. When the ball is moving along the lumen, it is difficult to have the ball moving along the surface without "sinking" into, or "hovering" over, the lumen in which the ROI cannot be marked. One way to address this is to emit a ray from the center of the ball, where

Fig. 1 Selection of surface points and the concept of GM. An object is created using threshold segmentation and the marching cubes algorithm. **a** A ray is emitted from the cursor to the object when the ball is moved using the cursor. The center of the ball (C) is updated continuously to keep the ray-object intersection (P) inside the radius of the ball. **b** Every vertex of a marching cubes triangle is on the edge of the voxel cube between voxels 1 and 2 representing the inside and outside the object. In our GM algorithm, the gray level of the voxel 1 is used as the gray level of the marching cubes vertex
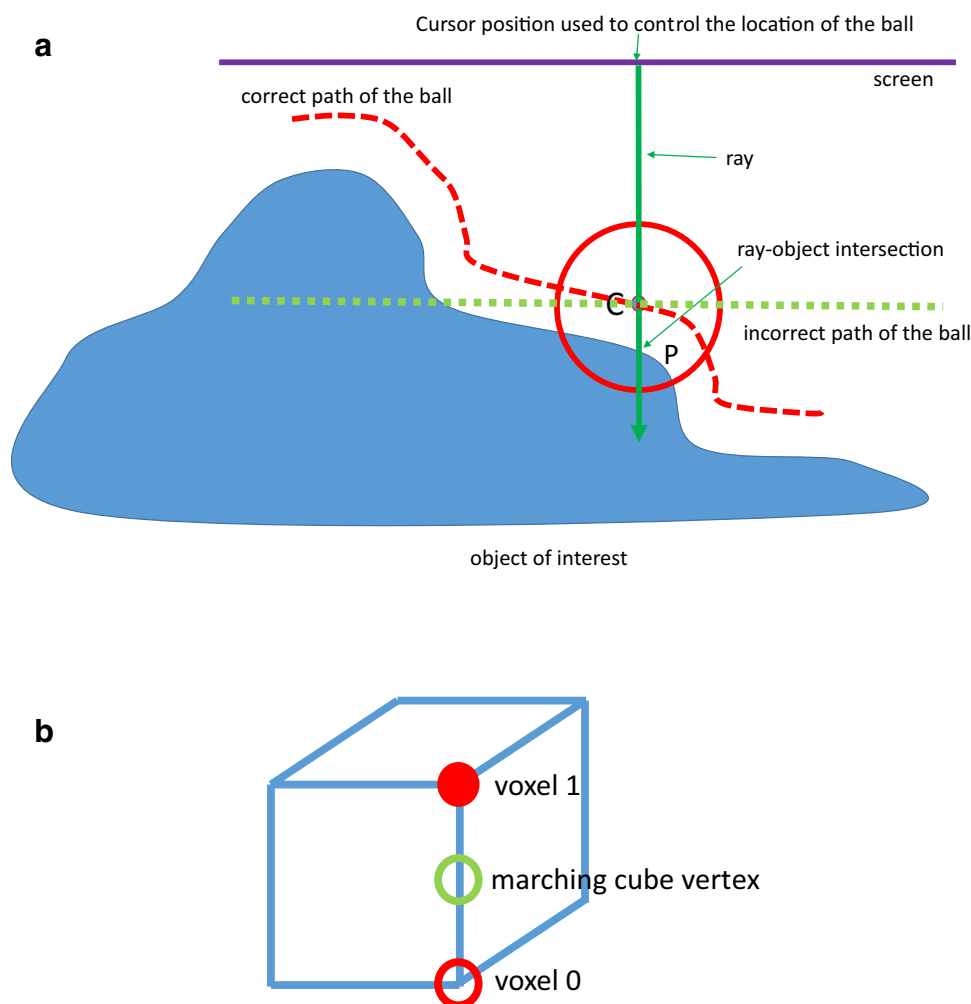
the current cursor is, toward the object. The intersection of the ray and the lumen is computed and shown in (Fig. 1a P). The radius of the ball that can be set by the user is R. We assume that the ball always "sinks" into the lumen about 50% of R. Therefore, the location of the center of the ball (Fig. 1a C) can be computed. As the ball is moving around, the C will be re-calculated and the ball will always "float" on the lumen properly. Once the center of the ball is determined, the vertices of the surface that are inside the ball can be efficiently computed. The color of all the vertices inside the ball is changed to a pre-set one and displayed (Fig. 2a).

2.5 GM of a Target ROI (TGM)

In the marching cubes algorithm, all the marching cubes vertices of the marching cubes triangles are on the edges of the 3D grid. The voxel 1 and voxel 0 represent two voxels with 1 and 0 values respectively in a binary object of interest, the internal and external voxels of the object (Fig. 1b). In our algorithm, the grey level of the marching cubes vertex takes the grey level of voxel 1, which is its closest internal voxel. This also reflects the fact that the grey level at the vertex represents the internal object surface. The vertices outside the ROI will remain unchanged. This technique can be implemented and run in real-time by use of a standard computer vision and graphics library, OpenGL or Direct3D. The ROI GM (i.e., TGM) is applied to CTC images and is compared with SR and GM. The visual effects of these are evaluated from a clinical point of view. For the display of original gray level information and comparison of SR, GM and TGM on the same basis, we did not apply special filters to remove noise and smooth CTC images, as commercial packages usually do. The only difference between SR and GM/TGM is whether the vertices are gray level mapped or not.

2.6 Clinical Evaluations

Two radiologists, A and B, each with more than 10 years of experience in reading abdominal CT were invited for the retrospective evaluation. They were asked to compare SR, GM, and TGM images simultaneously and then original CT images case-by-case. Both radiologists were blinded to the other's results. Three evaluation criteria were used for the evaluation of the target endoluminal lesions with SR, GM and TGM CTC images respectively: (1) 3D shape of the target; (2) surface texture and gray level pattern presentation, and; (3) the correlation between the 3D surface presentation and the original two dimensional (2D) CT images and 2D to 3D image correlation for lesion identification and

Fig. 2 Computed tomographic colonography (CTC) images of a 55-year-old male with a clinical diagnosis of rectal cancer. Comparison of SR, TGM and GM of colon cancer on CTC. **a** The process to decide the ROI. The semitransparent round ball (the red area) can be dragged by the user. The marked region (the green area) will be gray level mapped. **b** TGM of the polyp defined by (**a**) with the same view position and 3D position of the polyp (arrow). **c** The correlated 2D position of the polyp (cross) in the axial image. The HU is 51. The higher HU and smoother surface of the tumor compared to those of stool (Fig. 3b) can be seen more clearly and correlated well with 2D images in (**b**) but not in (**a**). **d** GM of CTC. The background scene is complicated by dense colonic fluid (arrow) and pericolonic fat (arrowhead)
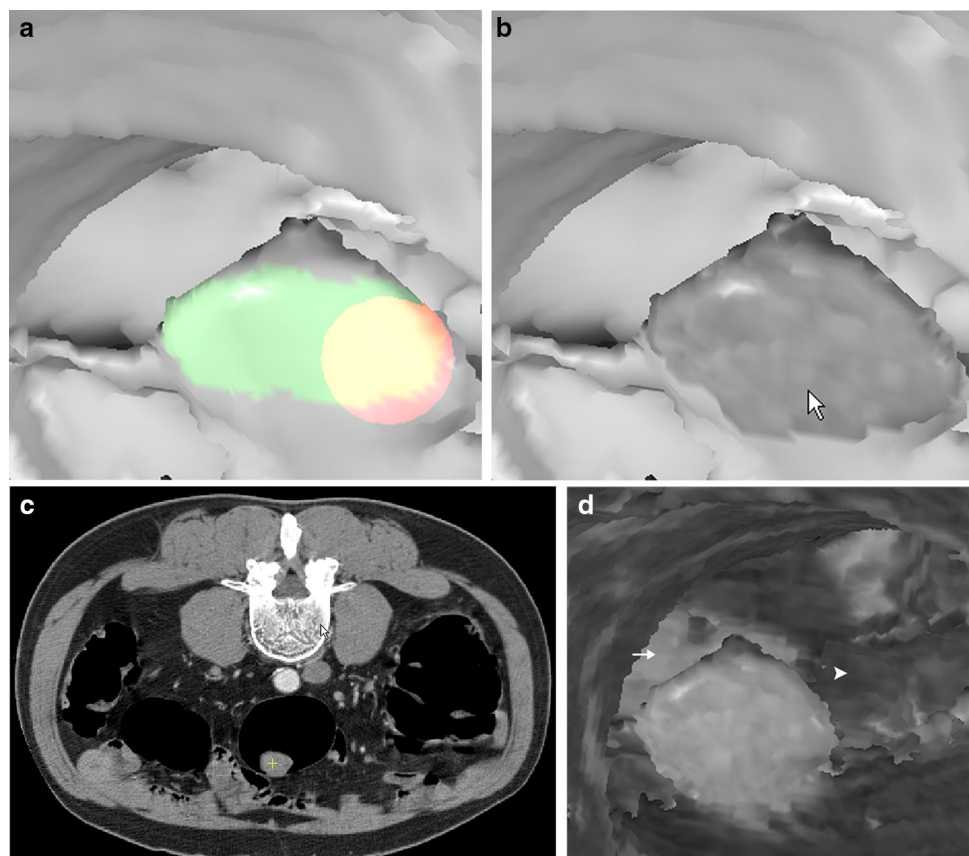
confidence classification (benignity and potential malignancy). A 3-point scale was used for the evaluation: score 1- poor (worse than SR); score 2- fair (equal to SR); and score 3- excellent (better than SR).

2.7 Diagnostic Performance

Two additional gastrointestinal radiologists, C and D, with 21 and 9 years of experience respectively, completed the clinical performance measurements of SR, GM and TGM images. The 3 types of images of each case were presented in random order to the radiologists. Images were evaluated in the same soft tissue window setting (window level, 40; window width, 400).

To simplify and evaluate only the 3D reconstructed views for CTC diagnosis, two radiologists were first asked to judge the lesions as to benignity or potential malignancy, using 3D SR, GM and TGM CTC images alone, without cross reference to the 2D images for study purposes only. The two radiologists were then asked to choose the preferable display mode for vision and differentiation of endoluminal lesions during the navigation. Both radiologists were also blinded to the other's results.

The Wilcoxon signed ranks test was used for data analysis in clinical evaluations. All statistical analyses were performed using the Statistical Package for the Social Sciences (SPSS) statistical software for Windows, version 22 (SPSS Inc., Chicago, USA). A probability ($P < 0.05$) was considered to indicate statistically significance.

3 Results

3.1 GM of a Target ROI (TGM)

Figures 2a, 3a, and 4a show traditional SR images of three polypoid lesions. The corresponding TGM images (Figs. 2b, 3b, and 4b) of the above polypoid lesions reveal an increased density polyp, heterogeneous low density stool, and very dense calcification/tagging agent. Figure 5a shows a prominent fold in a SR endoluminal view. The fat density of the fold lesion can be seen more clearly in TGM images (Fig. 5b, cross) than SR images (Fig. 5a). The 2D CT image

Fig. 3 A 75-year-old female with clinical history of bloody stool recently. Comparison of SR, TGM and GM of stool in CTC. **a** Traditional SR of CTC shows a polypoid lesion in the colon. **b** TGM of the above lesion shows more apparent rough surface, heterogeneous hypo-densities (cross) and the non-GM porous appearance (arrow) of stool. The features are easily obscured by the complex background in GM as shown in (**d**). **c** The corresponding 2D position (cross) of the hypo-densities in (**b** cross). Its HU is − 117. **d** GM of CTC
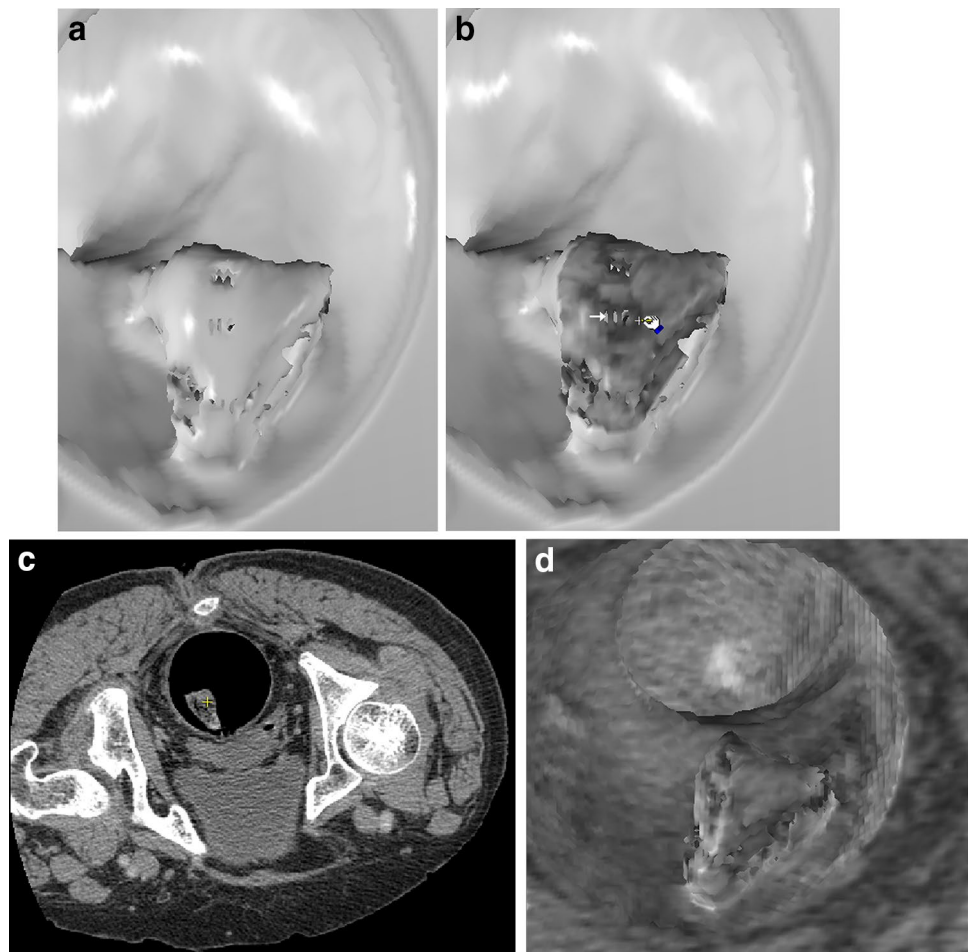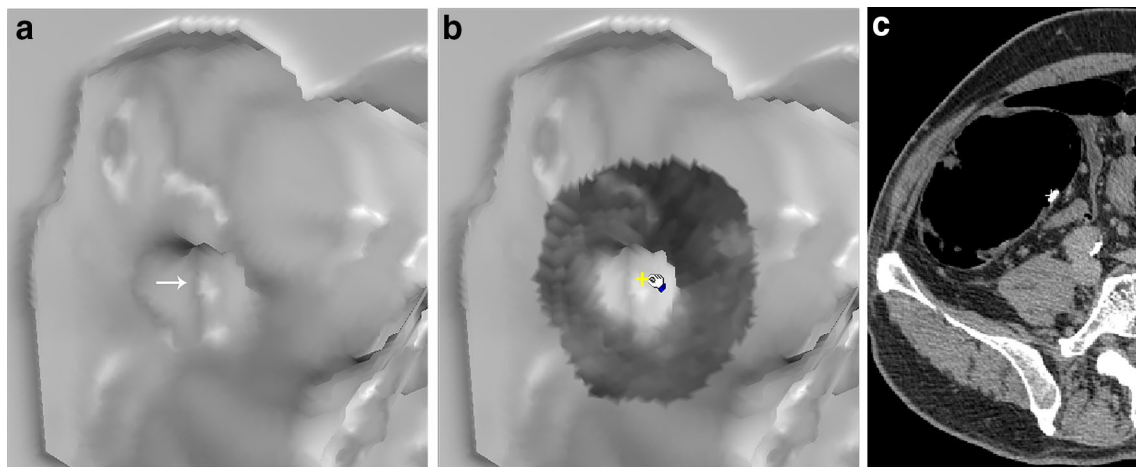
Fig. 4 A 60-year-old man underwent CT scanning due to sigmoid colon cancer found by colonography. CTC reveals a polypoid lesion in the ascending colon. Comparison of SR and TGM of the polyoid lesion on CTC. **a** Traditional SR of CTC shows a polypoid lesion (arrow) in the colon. **b** TGM of the polypoid lesion shows a calcification or tagging agent (cross) over the colon wall. **c** The correlated 2D point in the axial image (cross). Its HU is 325. The high density cannot be seen and correlated with 2D image in (**a**)

shows fat content of a lipomatous colon lesion (Fig. 5c). Figure 6a shows a SR endoluminal image with an irregularly flat area. The TGM image of the above area shows higher density tagged fluid (Fig. 6b, cross).

3.2 Clinical Evaluations

The preliminary reader scores of potentially malignant and benign conditions by the two radiologists, A and B, are shown in Fig. 7. TGM had significantly higher scores on surface texture and contour of endoluminal lesions than SR (one-tailed Wilcoxon signed ranks test: $P < 0.01$) (Table 1), as GM showed in Chen's article [6]. Moreover, TGM allows good correlation of 3D shape and gray level of any 3D point (the cross of Figs. 2b, 3b, 4b, 5b and 6b, for example) with its 2D image (the cross of Figs. 2c, 3c, 4c, 5c, 6c) and vice versa, while there is no gray level information of SR method to be correlated. The 3D to 2D and 2D to 3D correlation, lesion identification, and classification of TGM are significantly better than those of SR images ($P < 0.01$) (Table 1). TGM had an equal or higher score than GM in all criteria evaluated. The evaluation results of the two radiologists, A and B, were consistent with each other.

3.3 Diagnostic Performance

From the performance study of another two radiologists (C and D), SR, GM and TGM have high sensitivity (SR: 88.2–97.1% and GM, TGM: 100%) (Table 2). However, the specificity and diagnostic accuracy of TGM and GM methods are significantly better than those of SR, especially with regard to TGM (specificity: 75.0–85.7% vs. 14.3–17.9%; accuracy: 88.7–93.5% vs. 54.8–61.3%) ($P < 0.01$) (Table 2).

This shows that although SR, GM and TGM are very sensitive for detection of potential malignant endoluminal lesions, TGM and GM are much less likely to have false positive predictions and are more capable than SR of distinguishing benign from potentially malignant lesions. Distinguishing between TGM and GM, TGM performs better than GM at this point (specificity: 75.0–85.7% vs. 53.6–64.3%; accuracy: 88.7–93.5% vs. 77.4–83.9%) ($P < 0.01$) (Table 2). In general, TGM is higher than GM and GM is higher than SR with regard to sensitivity, specificity or diagnostic accuracy analysis.

For the applicability of screening navigation and target evaluation in CTC, both radiologists choose TGM but not GM as a preferable display mode in all cases.

4 Discussion and Conclusion

SR is the traditional display method on the 3D endoluminal view and provides very good 3D effect and efficient operation for the screening of endoluminal lesions. However, SR is not sufficient to display the nature of the intraluminal lesions for further differentiation. With TGM, the spatial effect of SR is maintained and an interactive tool adds corresponding gray level information to any 3D ROI. Thus, a direct 3D differentiation, or accurate point to point 3D to 2D image correlation, may be made in this ROI spatial gray level images.

The advantage of TGM is its native mapping of the CTE image using the gray levels of the original CT voxels contributing to the CTE. The interpretation of this type of gray level information is the same as most radiologists and physicians read with ordinary abdominal CT. TGM is also
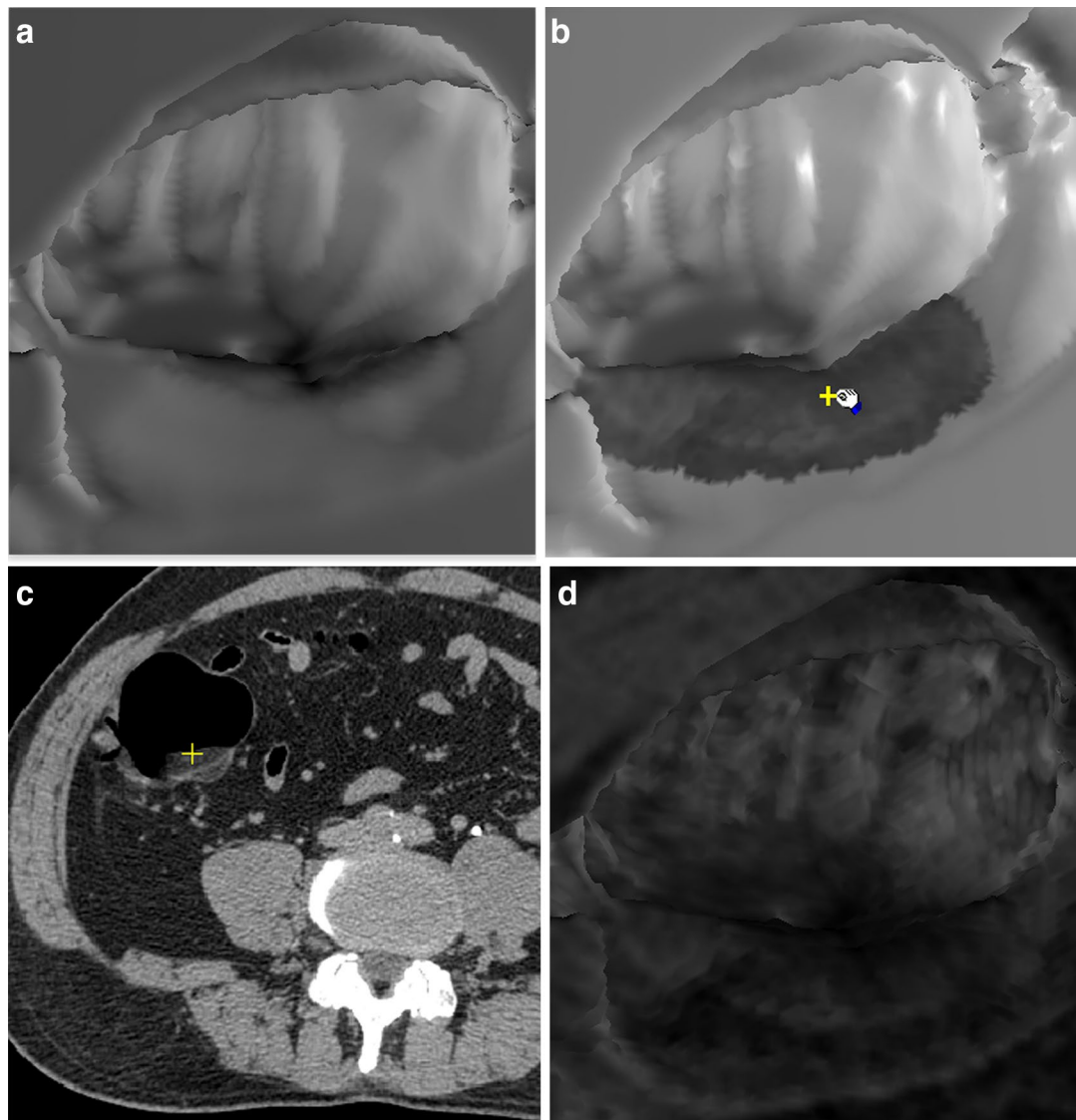
Fig. 5 Images of a 62-year-old male. Colonography revealed swelling of the ileocecal valve with narrowing of the terminal ileum in health examination. Comparison of SR, TGM and GM of the lipomatous area on CTC. **a** SR of a colonic lipomatous tumor. **b** TGM of the same tumor and a 3D interesting point (cross). **c** An axial CT image of a correlated colonic lipomatous area (cross). The cross in **b** shows a low HU (− 61) as fat density that cannot be seen in **a**. **d** Navigation and GM of a segment of colon in the same case. The heterogeneous background of shading, and gray level change, interfere with the detailed gray level evaluation of a target such as the lipomatous area (arrow) in this case

superior to VR due to the abstractive color mapping and difficulty in 2D correlation on VR images.

The interactive tool assists in evaluating interesting areas during navigation. The design of TGM allows the user to focus on the target lesion for further exploration, without interference by the gray level values in the background. Basically, GM and TGM have the same effect of gray level mapping, except that TGM can focus specifically on the target lesion, whereas GM maps the grey level values of the whole image. GM of the whole image interferes with the detailed evaluation of the gray level change of target lesion, especially in a complex background (Figs. 2d, 3d, and 5d), which is due to shading, fluid, density of normal colon wall or pericolonic fat, except for certain target dense calcifications or tagging agents (Figs. 4, 6). This is especially true while the user is navigating through a complicated environment such as the whole colon. Consequently, TGM got equal or higher scores in all clinical evaluation effects and was a preferable display model in CTC navigation. The specificity and diagnostic accuracy of TGM were also better than GM in the 3D diagnostic performance study. The results show
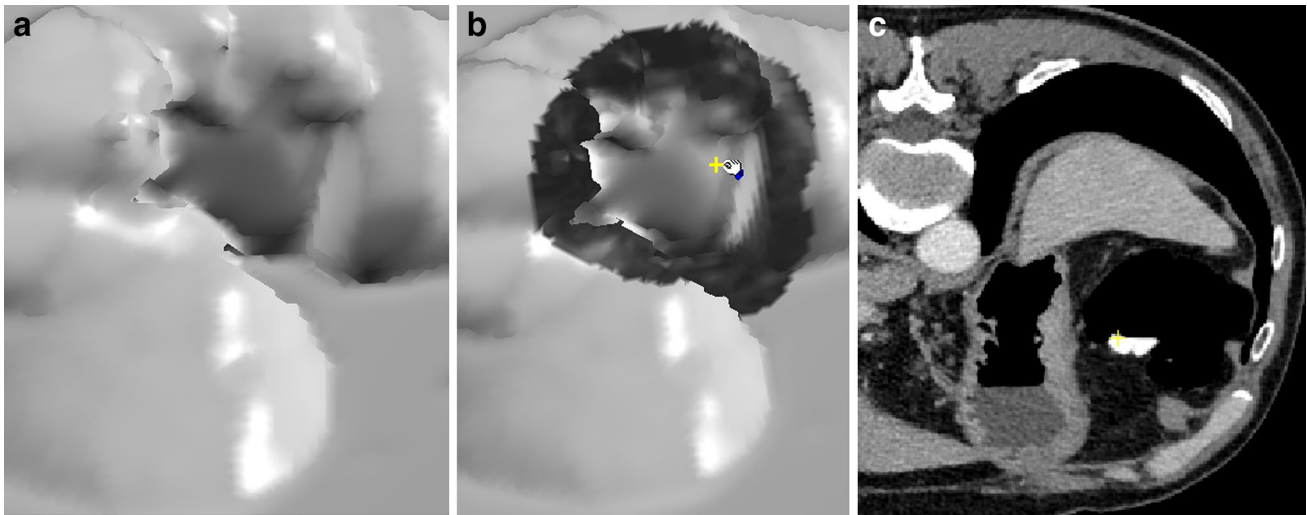
Fig. 6 CTC images of a 62-year-old man with colon cancer 20 cm from the anal verge. Comparison of SR, TGM of fluid and tagging effects in CTC. **a** SR of a CTC image shows an incidental irregularly flat lesion over the colon wall unrelated to the cancer. **b** TGM of the same lesion shows preservation of higher density nature of the tagged fluid (cross). **c** The original CT image. The cross indicates the corresponding 2D position of high density fluid tagging in **b**
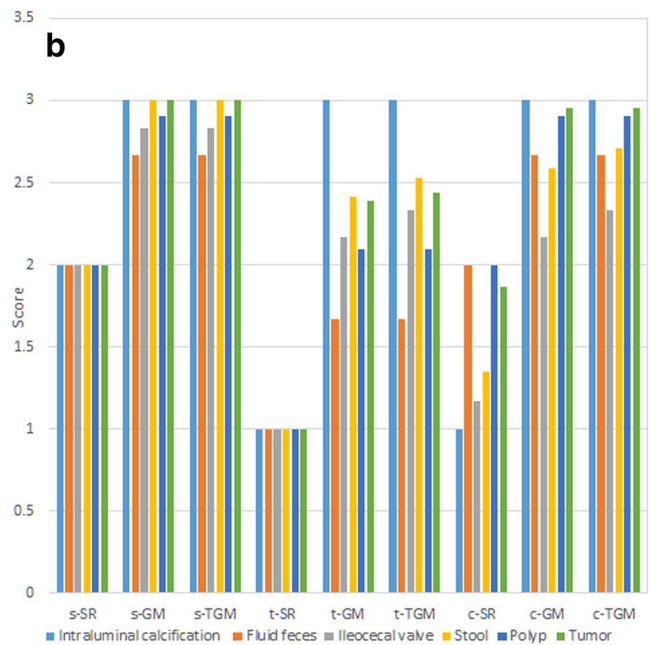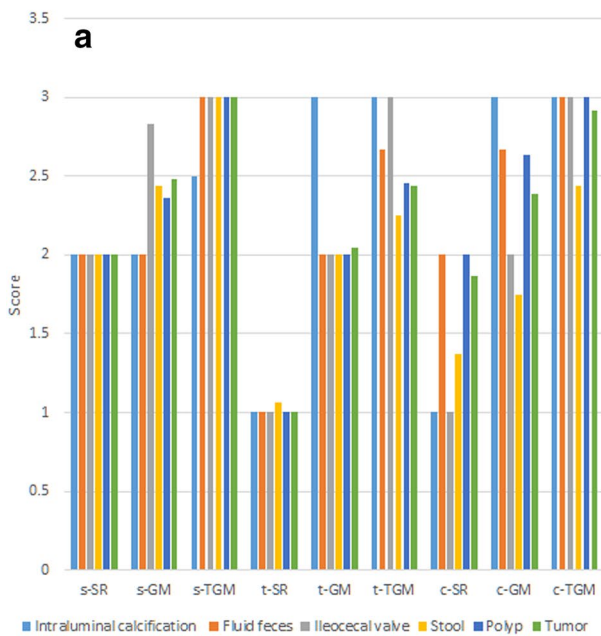

Fig. 7 Two readers' average scores of CTC: SR, GM and TGM. **a** Reader average score corresponding to the upper sub-row score in Table 1, **b** The other reader average score corresponding to the lower sub-row in Table 1. s-, t- and c- indicate shape, surface texture, correlation and classification scores. Both radiologists scored all classifications higher in GM and TGM than SR

TGM highlights the gray level mapping effect of the target lesion under a simple SR background.

Compared with SR, TGM images not only preserved the 3D shape of the non-target lesion region, but also significantly improved the gray level visualization of the target lesion region in virtual CTC ($P < 0.01$) (Figs. 2, 3, 4, 5, 6).

In addition, the user can correlate the 2D images by 3D shape, as well as by gray level information, to achieve better diagnosis and classification ($P < 0.01$). The user can double-check any 3D points of gray level mapping area with their counterparts in 2D images and, vice versa, simultaneously by the location and gray level value.

Table 1 Image features and classification scores of endoluminal lesions on CTC

Class	Case number	Rated feature	SR	GM	TGM	P value* vs. SR
Potential malignancy	34	Steric contour	2.00	2.44	3.00	< 0.01
			2.00	2.97	2.97	
		Surface texture	1.00	2.03	2.44	< 0.01
			1.00	2.29	2.32	
		2D correlation	1.91	2.47	2.94	< 0.01
		Classification	1.91	2.94	2.94	
Benignity	28	Steric contour	2.00	2.46	2.96	< 0.01
			2.00	2.93	2.93	
		Surface texture	1.03	2.07	2.5	< 0.01
			1.00	2.32	2.43	
		2D correlation	1.32	2.00	2.67	< 0.01
		Classification	1.35	2.54	2.64	

Potential malignancy: polyps or tumors

Benignity: stool, fluid feces, ileocecal valves, intraluminal calcification

Steric contour: 3D shape of the target

The upper and lower sub-rows of every rated feature indicate the average score of two different radiologists

*Wilcoxon signed ranks test (one-tailed)

Table 2 Diagnostic performance of SR, GM and TGM

Reviewer/display method	Sensitivity (95% CI)	Specificity (95% CI)	Diagnostic accuracy	P value*
Reader 1				
SR	97.1% (0.851, 0.995)	17.9% (0.079, 0.356)	61.3%	0.082
GM	100% (0.899, 1)	64.3% (0.458, 0.793)	83.9%	< 0.001
TGM	100% (0.899, 1)	85.7% (0.685, 0.943)	93.5%	< 0.001
Reader 2				
SR	88.2% (0.734, 0.953)	14.3% (0.057, 0.315)	54.8%	1.000
GM	97.1% (0.851, 0.995)	53.6% (0.358, 0.705)	77.4%	<0.001
TGM	100% (0.899, 1)	75.0% (0.566, 0.873)	88.7%	<0.001

CI confidence interval

*Values represent comparison between final pathology and diagnostic performance of SR, GM and, TGM

We explain each type of common CTC endoluminal lesion in the following: For tumor/polyps, higher soft tissue density, or increased densities of the tumor (Fig. 2b) due to contrast enhancement, can be seen on TGM CTC but not on SR images (Fig. 2a). The correlated position and higher gray level value in its 2D image are shown in (Fig. 2b arrow and 2c cross). For stool, the shaggy appearance and heterogeneous lower surface densities of stool due to no contrast enhancement and non-TGM porousness can be visualized in TGM (Fig. 3b), but not in SR images (Fig. 3a). The correlated 2D position and gray level value of the hypo-density in TGM image Fig. 3b (cross) is shown in Fig. 3c (cross). Its HU is − 117. For fat, if there is fat inside the protruding luminal area, it can be observed in TGM images (Fig. 5b), but not in SR images (Fig. 5a). The correlated 3D and 2D positions of fat content are shown in Fig. 5b and 5c (cross). Their HU values are − 61. Calcifications or tagging agents can be observed in TGM (Fig. 4b) and GM images, but cannot be differentiated in SR image (Fig. 4a). The corresponding 3D and 2D positions of the sample point are shown in Fig. 4b and c (cross). Its HU is 325. The homogeneous low-density nature of fluid, or high density nature of tagged fluid, is best observed in GM or TGM image (Fig. 6b).

Fecal and fluid tagging, to improve polyp detection, have become the prerequisite of CT colonography [11, 12]. TGM and GM are distinctly better ways to identify them than SR in CTC. For instance, the undetermined flat lesion in SR (Fig. 6a) is found to be fluid tagging with the TGM application (Fig. 6b).

3D endoluminal navigation such as CTC is an imaging technology that enables both 2D and 3D evaluation of the lesion. All reader and current consensus guidelines acknowledge the complementary role of both 2D and 3D visualization methods in CTC, and point-to-point correlation between the two is favored [13]. Studies favoring a solitary 2D interpretation over 3D viewing, yielded low sensitivities ranging from 55 to 64%, even for large polyps [14, 15]. In contrast, the primary 3D workup produced impressive results with up to 93.8% sensitivity for lesions > 10 mm [11]. However, primary 3D evaluation leads to an increased number of false-positive findings, thus decreasing specificity [16]. To avoid false-positive findings, applying an additional 2D workup of the suspected lesion in a primary 3D dataset evaluation is recommended [17]. Although most current CTC analysis software programs support simultaneous display of 3D and multi-planar 2D images, by placement of a cursor or mouse in either the 2D or 3D image, the voxel information of the 3D images (SR or VR) of the different locations can be shown. However, the information is difficult to differentiate and it is hard to do 3D and 2D image correlation. CTC readers must go back and forth from 3D to 2D, or 2D to 3D for image correlation to achieve adequate diagnosis. TGM facilitates this condition. TGM technique integrates the gray level information seen in 2D images into the 3D CTC image to represent air, calcification, contrast, enhancement, fat, non-enhancement feces and more. Therefore, different voxel locations reflect different gray level values of their corresponding points in the 2D image.

Previously, we needed to image the gray levels of the 3D spatial distribution of an endoluminal lesion by back and forth image correlation. But now, with TGM, we can do spatial and gray level mapping both at once, and see the gray level pattern directly in a 3D image. Our study concludes that radiologists can make an accurate 3D diagnosis, in most cases, using only TGM, with characteristic findings of calcifications, tagging agents, fat density, higher density or enhancing tumors, or shaggy, low density, non-GM porous stool (accuracy: 88.7–93.5%). However, accuracy of SR alone is only 54.8–61.3%. If readers find any region needs to be explored, they can trace it from 3D TGM CTC to 2D image or 2D to TGM image, as they prefer, to a point-to-point level by the location and gray level correspondence, as with GM, but more focused. This type of correlation is more precise and efficient than that of SR and VR because there is no gray level information on SR images, normally complex and abstract on VR images, whereas too many unrelated gray level information complicates GM images. Our study shows TGM facilitates 3D to 2D and 2D to 3D image correlation and classification, compared with SR during CTC reading (one-tailed Wilcoxon signed ranks test: P < 0.01).

Because there is always gray level information on the surface of endoluminal lesions, TGM can be applied to any layer going deeper into the surface, if layer-by-layer examination can be performed by surface erosion methods. The same 3D and 2D image correlation can be performed inside the endoluminal lesions, just as it applies on the surface for further differentiation. Due to lack of gray level information, the correlation in the deeper layer is virtually impossible in SR images. TGM also makes the gray level and texture-based studies feasible for computer-aided detection and spatial localization of benign and malignant pathology.

To test the TGM effect in the non-contrast images, one of the cases with proven colon cancer, and impacted stool without intravenous contrast administration, was selected to reconstruct the 3D images and demonstrate the effects. These CTC images are shown in Fig. 8. Similar to the contrast CTC images in Figs. 2 and 3, tumors show higher soft tissue density with smooth surface (Fig. 8b, arrow), whereas stool shows heterogeneous lower densities (Fig. 8b cross) with shaggy and porous appearance. As we can see from the figures, TGM can reflect the gray level patterns of endoluminal lesions, no matter whether they are the contrast or non-contrast images. However, the contrast material can increase the gray level difference between the enhancing and non-enhancing lesions. If there are significant attenuation differences of lesions in the CT images, or a screening purpose, TGM of non-contrast CT is sufficient. On the contrary, if there are no significant attenuation differences or diagnostic purposes, TGM of contrast CT is best utilized to improve diagnostic accuracy.

We note two limitations of this study. One is that because the objects are displayed using the graphics processing unit in the display card, the 3D shading algorithm is always applied to the 3D object surface automatically by the hardware (although we have adjusted some parameters to reduce this shading effect). Therefore, the TGM to the 3D surface is still affected by the shading values. The other limitation is that we only evaluated the gray level information of the surfaces of endoluminal lesions, which are easily affected by the tagging agents and/or air densities. The correlations between the 3D and 2D images of special attenuation points below the surface are difficult and not accessible in the ordinary CTE analysis. Exploration of the gray level changes of the specific contents below the surface by TGM and surface erosion methods will be addressed in future studies to further facilitate discrimination of endoluminal lesions.

In conclusion, a novel TGM 3D endoluminal display technique is presented in this study. It is simple, concise and easy to implement. Compared with the monochrome spatial

Fig. 8 Noncontrast CTC Images of a 74-year-old female with a descending colon cancer. **a** An SR image of an annular colon mass and a proximal impacted polypoid lesion. **b** TGM of **a** shows higher density and smooth surface of the mass (arrow). The findings are similar to the contrast Fig. 2b image and colon cancer was confirmed. The polypoid lesion proximal to the above mass shows heterogeneous lower densities (cross) with shaggy and porous appearance. It proved to be stool with similar findings of the contrast Fig. 3b image
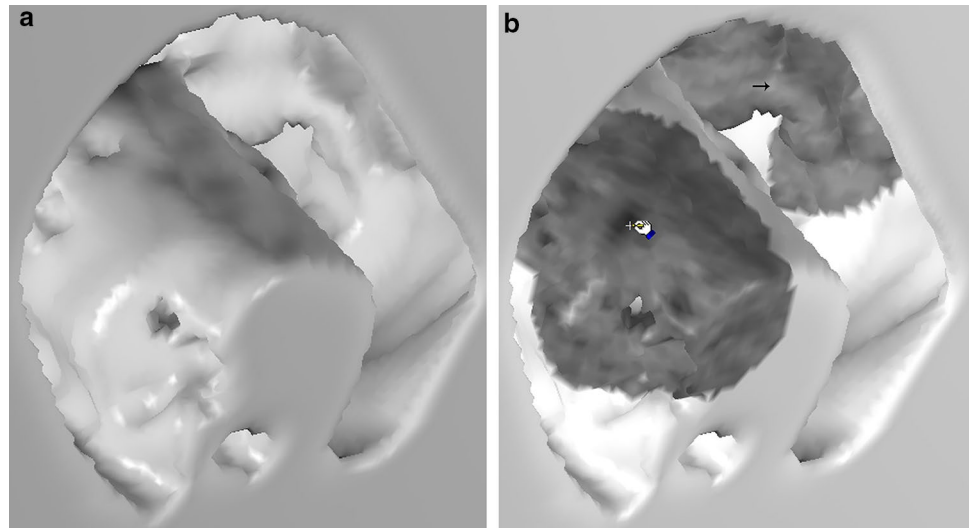
effect of traditional SR, 3D gray level endoluminal images can be provided by TGM. At the same time, 2D–3D image correlations are also increased and facilitated. Preliminary clinical evaluation by the two radiologists, C and D, shows TGM has the same sensitivity but a much lower false positive prediction. TGM has less interference of the background shading and gray level change commonly seen in GM. TGM serves as a more suitable tool for further evaluation of endoluminal lesions in 3D CTC reading. It is anticipated that TGM will be further applied to the exploration of endoluminal lesions and that there will be additional investigation of TGM's application in other tubular systems, such as with airway disease, and with other applications of endoscopy.

References

1. Siegel, R. L., Miller, K. D., Fedewa, S. A., et al. (2017). Colorectal cancer statistics. *CA: A Cancer Journal for Clinicians, 67,* 177–193.
2. Dominitz, J. A., Eisen, G. M., Baron, T. H., et al. (2003). Complications of colonoscopy. *Gastrointestinal Endoscopy, 57*(4), 441–445.
3. Heath, D. G., Soyer, P. A., Kuszyk, B. S., et al. (1995). Three-dimensional spiral CT during arterial portography: Comparison of three rendering techniques. *Radiographics, 15*(4), 1001–1011.
4. Pickhardt, P. J. (2004). Translucency rendering in 3D endoluminal CT colonography: A useful tool for increasing polyp specificity and decreasing interpretation time. *American Journal of Roentgenology, 183*(2), 429–436.
5. Macari, M., & Megibow, A. J. (2001). Pitfalls of using three-dimensional CT colonography with two-dimensional imaging correlation. *AJR. American Journal of Roentgenology, 176*(1), 137–143.
6. Chen, L. S., Hsu, T. W., Chen, S. J., et al. (2017). Application of gray level mapping in computed tomographic colonography: A

pilot study to compare with traditional surface rendering method for identification and differentiation of endoluminal lesions. *British Journal of Radiology, 90*(1070), 20160733.
7. Park, S. H., Lee, S. S., Kim, J. K., et al. (2008). Volume rendering with color coding of tagged stool during endoluminal fly-through CT colonography: Effect on reading efficiency. *Radiology, 248*(3), 1018–1027.
8. Liedenbaum, M. H., et al. (2010). CT colonography with minimal bowel preparation: Evaluation of tagging quality, patient acceptance and diagnostic accuracy in two iodine-based preparation schemes. *European Radiology, 20*(2), 367–376.
9. Valev, V., Wang, G., & Vannier, M. W. (1999). Techniques of CT colonography (virtual colonoscopy). *Critical Reviews in Biomedical Engineering, 27*(1–2), 1–25.
10. Lorensen, W. E., Cline, H. E. (1987). Marching cubes: A high resolution 3D surface construction algorithm. In *SIGGRAPH '87 proceedings of the 14th annual conference on computer graphics and interactive techniques. ACM, 21*(4), 163–169.
11. Pickhardt, P. J., Choi, J. R., Hwang, I., et al. (2003). Computed tomographic virtual colonoscopy to screen for colorectal neoplasia in asymptomatic adults. *New England Journal of Medicine, 349*(23), 2191–2200.
12. Johnson, C. D., Chen, M. H., Toledano, A. Y., et al. (2008). Accuracy of CT colonography for detection of large adenomas and cancers. *New England Journal of Medicine, 359,* 1207–1217.
13. Dachman, A. H., & Laghi, A. (2010). *Atlas of virtual colonoscopy.* Berlin: Springer.
14. Cotton, P. B., Durkalski, V. L., Pineau, B. C., et al. (2004). Computed tomographic colonography (virtual colonoscopy): A multicenter comparison with standard colonoscopy for detection of colorectal neoplasia. *JAMA, 291*(14), 1713–1719.
15. Rockey, D. C., Paulson, E., Niedzwiecki, D. E., et al. (2005). Analysis of air contrast barium enema, computed tomographic colonography, and colonoscopy: Prospective comparison. *The Lancet, 365*(9456), 305–311.
16. Pickhardt, P. J. (2007). Screening CT colonography: How I do it. *American Journal of Roentgenology, 189*(2), 290–298.
17. Schmidt, S. A., Ernst, A. S., Beer, M., et al. (2015). 3D detection of colonic polyps by CT colonography: Accuracy, pitfalls, and solutions by adjunct 2D workup. *Clinical Radiology, 70*(10), 1144–1151.

Affiliations

Lih-Shyang Chen[1] · Ta-Wen Hsu[2,3] · Shao-Jer Chen[3,4,9] · Shu-Han Chang[1] · Chih-Wen Lin[3,4] · Yu-Ruei Chen[3,4] · Chin-Chiang Hsieh[5] · Shu-Chen Han[6] · Ku-Yaw Chang[7] · Chun-Ju Hou[8]

[1] Department of Electric Engineering, National Cheng Kung University, Tainan, Taiwan, ROC

[2] Department of General Surgery, Dalin Tzu Chi Hospital, Buddhist Tzu Chi Medical Foundation, Chiayi, Taiwan, ROC

[3] School of Medicine, Tzu Chi University, Hualien, Taiwan, ROC

[4] Department of Medical Imaging, Dalin Tzu Chi Hospital, Buddhist Tzu Chi Medical Foundation, Chiayi, Taiwan, ROC

[5] Department of Radiology, Tainan Hospital, Ministry of Health and Welfare, Tainan, Taiwan, ROC

[6] Department of Radiology, Tainan Municipal Hospital, Tainan, Taiwan, ROC

[7] Department of Computer Science and Information Engineering, Da-Yeh University, Changhua, Taiwan, ROC

[8] Department of Electrical Engineering, Southern Taiwan University of Science and Technology, Tainan, Taiwan, ROC

[9] Department of Medical Imaging, Buddhist Dalin Tzu Chi General Hospital, No. 2, Min-Sheng Road, Dalin Town, Chiayi 622, Taiwan, ROC